MATHEMATICS IN ENGINEERING, SCIENCE AND AEROSPACE
MESA - www.journalmesa.com
Vol. 1, No. 2, pp. 119-138, 2010

Aeroelastic oscillations of a delta wing with bonded piezoelectric strips in supersonic flow

D. Mateescu*, A. K. Misra, S. Shrivastava

Department of Mechanical Engineering, McGill University
817 Sherbrooke Street West, Montreal, QC, Canada. H3A2K6.

* *Corresponding Author*. E-mail address: dan.mateescu@mcgill.ca

Abstract. Aeroelastic oscillations of a delta wing are studied under the combined effects of unsteady supersonic aerodynamic loading and voltages applied to bonded piezoelectric strips. The delta wing is modelled as a cantilevered triangular plate undergoing small transverse oscillations. A hybrid analytical-numerical method is developed for the unsteady supersonic aerodynamics of the wing in order to determine the pressure distribution and the generalized aerodynamic forces on the wing. Transient and harmonic responses of the wing, in the presence of piezoelectric strips, are calculated for both with and without aerodynamic loading. It is found that the aeroelastic oscillations can be effectively reduced by applying particular combinations of voltages in a small number of piezoelectric strips. It is observed that piezoelectric actuators aligned with the span direction are more effective than the chord-aligned piezoelectric actuators, which produce little or no reduction in oscillations.

1 Introduction

Aeroelastic oscillations of the wings play an important role in the design of an aircraft. Instabilities associated with these oscillations, such as flutter of wings, affect the maximum flight speed. Suppression of these oscillations is important in order to increase the flight envelope as well as to improve the safety of the structure. Flutter suppression is especially important for supersonic wings. Controlling aeroelastic oscillations also helps in providing smoother rides and lower root loads.

Aeroelastic oscillations of a wing can be controlled by passive or active means. The problems associated with the conventional control methods include large added weight, hydraulic lag and high cost. Researchers are currently looking at smart materials as an alternative to the conventional control surface actuation. Piezoelectric or piezoceramic materials can be used as strain actuators. These can easily be integrated onto the surface of the wing in the form of thin layers or individual strips. Delta wings, i.e. wings of symmetrical triangular form, are used commonly on supersonic aircraft. Hence,

2010 **Mathematics Subject Classification**: 76J20, 74H45, 76G25, 74B05, 74B20.
Keywords: Delta wings, Supersonic flows, Aeroelastic oscillations, Piezoelectric actuators.

examination of aeroelastic oscillations of delta wings subjected to supersonic flow and study of their suppression are of practical interest.

There is a large body of literature dealing with the active control of structures using piezoelectric/piezoceramic actuators. This will not be reviewed here; any interested reader can find the relevant information in several books (e.g., Srinivasan and McFarland [1]). On the other hand, there is a small number of studies [2-6] dealing with active flutter suppression of panels and certain wing planforms using piezoelectric materials. None of these studies, however, considers a delta wing subjected to unsteady aerodynamic loads caused by supersonic flight.

The work presented herein is multi-disciplinary involving structural analysis of a delta wing, aerodynamic modelling, and then a coupling of the two models to study the response of the delta wing under the combined aerodynamic and piezoelectric forces. The development of an active suppression model necessitates a convenient, efficient and accurate aerodynamic model that can be easily combined with the structural-piezoelectric model of the delta wing. Specifically, the objective of this paper is to study the aeroelastic oscillations of a delta wing under unsteady supersonic loading in the presence of bonded piezoelectric strips. The dynamic response of the delta wing is found using a combination of analytical and numerical techniques. The work is carried out in three steps: (i) modeling of the uncontrolled, unloaded structure; (ii) modeling of the uncontrolled but aerodynamically loaded structure; and (iii) modeling of the structure in the presence of both aerodynamic and piezoelectric loading. The following consists of a concise exposition of the three modelling steps, plus a presentation of the results.

2 Structural modelling

This section describes the structural modelling of the delta wing without aerodynamic loading or piezoelectric forces. This uncontrolled structural model will be referred to as the “free –system”. As shown in Figure 1, l is the semi-span of the wing along the x-axis, and c is the chord of the wing along the y-axis. The z-axis is normal to x- and y-axes. The delta wing is assumed to be a thin plate of uniform thickness, h_p . It is also assumed that the wing is symmetrical and each half-wing is fixed at the central chord.

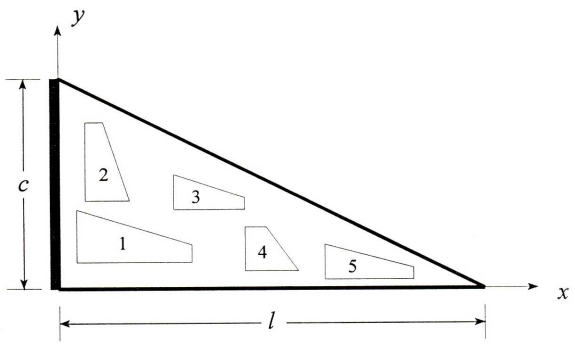

Fig. 1 Distribution of PVDF strips on a half of a delta wing modelled as a cantilevered triangular plate

The mass and stiffness matrices of the delta wing are derived in this paper using the energy approach, starting from the first principles. The general expressions for the kinetic and potential energy are:

$$T = \frac{1}{2}\int_A m\left(\frac{\partial w}{\partial t}\right)^2 dA \quad , \tag{2.1}$$

$$V = \frac{D}{2}\int_A \left[\left(\frac{\partial^2 w}{\partial x^2}+\frac{\partial^2 w}{\partial y^2}\right)^2 - 2\,(1-\nu)\left\{\frac{\partial^2 w}{\partial x^2}\frac{\partial^2 w}{\partial y^2}-\left(\frac{\partial^2 w}{\partial x\,\partial y}\right)^2\right\}\right] dA \quad , \tag{2.2}$$

where w is the transverse displacement of an arbitrary point on the cantilevered plate; m is the mass per unit area; and v is the Poisson's ratio. The flexural rigidity of the plate, D , is given by

$$D = E_P h_P^3/12(1-\nu^2) \quad , \tag{2.3}$$

where E_P and h_p are the Young's modulus and the thickness of the plate, respectively. The two energy expressions can be used to obtain a boundary value problem that describes the free vibration of the plate.

2.1 Discretization of the wing

A general closed-form solution of the free (or forced) vibration problem does not exist in this case due to the non-uniform mass and stiffness distribution of a triangular plate. Therefore, an approximate method, namely the *Assumed Modes Method*, is used to generate the mass and stiffness matrices of the discretized system. This method assumes a solution of the boundary-value problem in the following form:

$$w(x,y,t) = \sum_{r=1}^{M}\sum_{s=1}^{N}\Phi_r(x)\Psi_s(y)q_{rs}(t) \quad , \tag{2.4}$$

where the transverse displacement w is expanded in terms of a set of shape functions; q_{rs} is the generalized displacement; Φ_r and Ψ_s are shape functions chosen along the x and y directions (clamped-free and free-free directions), respectively; and M and N are the number of clamped-free and free-free shape functions, respectively. The chosen shape functions are admissible functions, that is, they need to satisfy only the geometric boundary conditions. The *Assumed Mode Method* uses equation (2.4) in conjunction with Lagrange's equations of motion to obtain a formulation leading to an approximate solution of the associated eigenvalue problem. Equation (2.4) can be substituted in the kinetic and potential energy equations to generate mass and stiffness matrices of the discretized system. Using non-dimensional spatial co-ordinates, equation (2.4) can be re-written as,

$$w(\xi,\eta,t) = \sum_{r=1}^{M}\sum_{s=1}^{N}\Phi_r(\xi)\Psi_s(\eta)q_{rs}(t) \quad , \tag{2.5}$$

where ξ and η are non-dimensional coordinates in the x- and y-directions respectively and are defined as

$$\xi = x/l, \quad \eta = (y/c)/(1-x/l) \quad , \tag{2.6}$$

The clamped-free and free-free shape functions for the plate are chosen respectively in the form

$$\Phi_r(\xi) = \xi^{r+1} \quad , \tag{2.7}$$

$$\Psi_s(\eta) = \left[(1-\xi)^2(-\eta+1/2)\right]^{s-1} \quad , \tag{2.8}$$

substituting equations (2.5)- (2.8) into equation (2.1), the kinetic energy expression can be written as

$$T = \frac{1}{2}\sum_{i=1}^{MN}\sum_{j=1}^{MN} m_{ij}\dot{q}_i\dot{q}_j = \frac{1}{2}\{\dot{q}\}^T [M]\{\dot{q}\} \quad , \tag{2.9}$$

where m_{ij} are the elements of the mass matrix and are given by

$$m_{ij} = \rho h_P c l \int_0^1\int_0^1 (1-\xi)\Phi_r(\xi)\Psi_s(\eta)\Phi_k(\xi)\Psi_p(\eta)\,d\xi d\eta \quad , \tag{2.10}$$

and where $i = (r-1)N + s$, $j = (k-1)N + p$, r, k = 1,...,M , and s, p = 1,...,N . Thus, the mass matrix of a cantilevered triangular plate has been obtained.

The stiffness matrix is determined by a similar procedure. By substituting equations (2.5) – (2.8) into equation (2.2), the potential energy expression can be written as

$$V = \frac{1}{2}\sum_{i=1}^{MN}\sum_{j=1}^{MN} k_{ij}\dot{q}_i\dot{q}_j = \frac{1}{2}\{\dot{q}\}^T [K]\{\dot{q}\} \quad , \tag{2.11}$$

where i and j are as defined earlier.

The expressions for k_{ij} are given in Appendix A. Both mass and stiffness matrices for the "free-system" have now been obtained.

2.2 Generalized forces

The two types of external forces acting on the system are those due to the aerodynamic loading and piezoelectric forces. Using Lagrange's equations for non-conservative systems, the equation for the dynamic system can be written as

$$[M]\ \{\ddot{q}\} + [C]\ \{\dot{q}\} + [K]\ \{q\} = \{Q_{aero}\} + \{Q_{piezo}\} \quad , \tag{2.12}$$

where $[M]$ is the mass matrix, $[C]$ is the structural damping matrix, $[K]$ is the stiffness matrix, and $\{Q_{aero}\}$ and $\{Q_{piezo}\}$ are the generalized forces due to the unsteady supersonic aerodynamic loading and the controlling action of the PVDF strips, respectively. The structural damping modelled here as *Rayleigh damping*, can be written as

$$[C] = \alpha[M] + \beta[K] \quad , \tag{2.13}$$

where α and β are plate material constants. For later reference, equation (2.12) can be written in state-space form as

$$\{\dot{x}\} = [A]\ \{x\} + [B]\ \{F\} \quad , \tag{2.14}$$

where $\{x\}$ is the state vector constructed form the generalized displacements and their time derivatives, and $\{F\}$ is the forcing vector.

The expressions for $\{Q_{aero}\}$ and $\{Q_{piezo}\}$ are derived in the following sections.

3 Aerodynamic modelling

The delta wing of central chord c and semi-span l is assumed to be situated in a uniform supersonic airstream of Mach number $M_\infty = U_\infty / a_\infty > 1$, where U_∞ is the velocity of the uniform airstream and a_∞ is the speed of sound that can be expressed as a function of the static pressure p_∞ and the density ρ_∞ of the undisturbed uniform airstream, $a_\infty = \sqrt{\gamma p_\infty / \rho_\infty}$, in which γ is the specific heat ratio (1.4 for air).

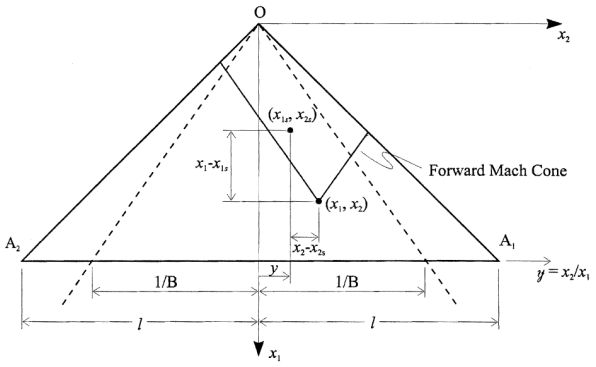

Fig. 2 Geometry of the delta wing in supersonic flow with the Mach cone represented by interrupted line and the forward Mach cone by solid line.

For the aerodynamic analysis, the flow past the delta wing is referred to the system of reference $Ox_1x_2x_3$ shown in Figure 2, where x_1, x_2, x_3 are nondimensional coordinates (nondimensionalized with respect to the chord c) that are related to the coordinates x , y used in the structural analysis by the equations

$$x_1 = (c - y)/c \quad , \quad x_2 = x/c \quad . \tag{3.1}$$

The general equation of the perturbation velocity potential for the unsteady supersonic flow past the oscillating delta wing, $\varphi(x_1, x_2, x_3, t) = \phi(x_1, x_2, x_3, t) - U_\infty x_1$, can be expressed in the linear form [7, 8] as

$$-B^2 \frac{\partial^2 \varphi}{\partial x_1^2} + \frac{\partial^2 \varphi}{\partial x_2^2} + \frac{\partial^2 \varphi}{\partial x_3^2} = c^2 \frac{M_\infty^2}{U_\infty^2} \left(\frac{\partial^2 \varphi}{\partial t^2} + \frac{2U_\infty}{c} \frac{\partial^2 \varphi}{\partial x_1 \partial t} \right) \quad , \quad B = \sqrt{M_\infty^2 - 1} \quad , \tag{3.2}$$

and the unsteady pressure coefficient C_p is derived from the Bernoulli-Lagrange equation [7, 8] in the form

$$C_p = \frac{p - p_\infty}{\frac{1}{2}\rho_\infty U_\infty^2} \quad \Rightarrow \quad C_p = -\frac{2}{U_\infty^2} \left(\frac{\partial \varphi}{\partial t} + \frac{U_\infty}{c} \frac{\partial \varphi}{\partial x_1} \right) \quad . \tag{3.3}$$

3.1 Aerodynamic problem formulation and solution for the delta wing

The delta wing with supersonic leading edges ($Bl > 1$) is assumed to execute low-frequency harmonic oscillations defined by the following equation in complex form of the wing surface

$$x_3 = h(x_1, x_2, t) = \hat{h}(x_1, x_2) \, \exp(i\omega t) \quad , \tag{3.4}$$

where ω is the radian frequency of oscillations ($\omega = 2\pi f$ where f is the oscillation frequency in Hz), $\hat{h}(x_1, x_2)$ is a function of the spatial coordinates and $i = \sqrt{-1}$. In this case, the boundary condition on the oscillating wing (for $x_3 \approx 0$) can be expressed in the form

$$\frac{\partial \varphi}{\partial x_3} = c^2 \left(\frac{\partial h}{\partial t} + \frac{U_\infty}{c} \frac{\partial h}{\partial x_1} \right) \quad \Rightarrow \quad \frac{\partial \varphi}{\partial x_3} = c \left(i\omega c \hat{h}(x_1, x_2) + U_\infty \frac{\partial \hat{h}}{\partial x_1} \right) \exp(i\omega t) \quad , \tag{3.5}$$

This condition is complemented by the boundary conditions on the plane $x_3 = 0$ outside the wing [7, 8] expressed as

$$\frac{\partial \varphi}{\partial x_1} = \frac{\partial \varphi}{\partial x_2} = 0 \quad , \quad \varphi = 0 \quad . \tag{3.6}$$

As a result, the perturbation velocity potential $\varphi(x_1, x_2, x_3, t)$, satisfying the differential equation (3.2), is also a harmonic function of the same frequency ω .

Consider the reduced velocity potential $\hat{\varphi}(x_1, x_2, x_3)$ defined by the following transformation of the perturbation velocity potential $\varphi(x_1, x_2, x_3, t)$

$$\varphi(x_1, x_2, x_3, t) = c U_\infty \hat{\varphi}(x_1, x_2, x_3) \exp(i\omega t + i k x_1) \quad . \tag{3.7}$$

where k has the expression

$$k = -\lambda \frac{M_\infty^2}{M_\infty^2 - 1} = -\lambda \frac{M_\infty^2}{B^2} \quad , \quad \lambda = \frac{\omega c}{U_\infty} \quad , \tag{3.8}$$

in which λ is the reduced frequency of oscillations. After this transformation, the governing equation (3.2) becomes a partial differential equation independent of time in terms of the reduced velocity potential $\hat{\varphi}(x_1, x_2, x_3)$ in the form

$$-B^2 \frac{\partial^2 \hat{\varphi}}{\partial x_1^2} + \frac{\partial^2 \hat{\varphi}}{\partial x_2^2} + \frac{\partial^2 \hat{\varphi}}{\partial x_3^2} = \lambda^2 \frac{1 + B^2}{B^2} \hat{\varphi}(x_1, x_2, x_3) \quad . \tag{3.9}$$

The unsteady pressure coefficient C_p can be expressed in this case as

$$C_p(x_1, x_2, x_3, t) = \hat{C}_p(x_1, x_2, x_3) \exp(i\omega t) \quad , \tag{3.10}$$

where the reduced pressure coefficient is defined in the form

$$\hat{C}_p(x_1, x_2, x_3) = -2 \left[i(k + \lambda) \hat{\varphi}(x_1, x_2, x_3) + \frac{\partial \hat{\varphi}}{\partial x_1} \right] \exp(i k x_1) \quad . \tag{3.11}$$

The boundary condition (3.5) on the oscillating wing can now be expressed in terms of the reduced potential $\hat{\varphi}(x_1, x_2, x_3)$ in the form

$$\frac{\partial \varphi}{\partial x_3} = c U_\infty \frac{\partial \hat{\varphi}}{\partial x_3} \exp(i\omega t + i k x_1) \quad \Rightarrow \quad \frac{\partial \hat{\varphi}}{\partial x_3} = \hat{W}(x_1, x_2) \exp(-i k x_1) \quad , \tag{3.12}$$

where

$$\hat{W}(x_1, x_2) = i\lambda \hat{h}(x_1, x_2) + \frac{\partial \hat{h}}{\partial x_1} \quad . \tag{3.13}$$

which is complemented by the boundary conditions (3.6) on the plane $x_3 = 0$ outside the wing that is expressed in the form

$$\frac{\partial \hat{\varphi}}{\partial x_1} = \frac{\partial \hat{\varphi}}{\partial x_2} = 0 \quad , \quad \hat{\varphi} = 0 \quad . \tag{3.14}$$

The solution of the differential equation (3.9) with second-order partial derivatives subject to the boundary conditions (3.12) and (3.14) can be obtained by using the pulsating source concept. Consider first the potential of a source situated at the point $S(x_{1S}, x_{2S}, x_{3S} = 0)$ in steady supersonic flow that is defined [7, 8] in the form

$$\hat{\varphi}_S(x_1, x_2, x_3) = \hat{\varphi}_S(R) \quad \text{where} \quad R = \sqrt{(x_1 - x_{1S})^2 - B^2 (x_2 - x_{2S})^2 - B^2 x_3^2} \tag{3.15}$$

which satisfies equation (3.9) for $\lambda = 0$ (steady case). Inserting the reduced velocity potential $\hat{\varphi}_S(x_1, x_2, x_3) = \hat{\varphi}_S(R)$ in (3.9) one obtains the ordinary differential equation

$$\frac{d^2 \hat{\varphi}_S}{dR^2} + \frac{2}{R} \frac{d\hat{\varphi}_S}{dR} - \frac{K^2}{B^2} \hat{\varphi}_S(R) = 0 \quad , \tag{3.16}$$

where

$$K = \lambda \frac{M_\infty}{B} \quad \Rightarrow \quad k = -K \frac{M_\infty}{B} \quad , \tag{3.17}$$

A solution of this differential equation is

$$\hat{\varphi}_S(R) = \frac{1}{R} \cos\left(\frac{K}{B} R\right) \quad , \tag{3.18}$$

which leads to the following expression of the velocity potential of the pulsating source of unit intensity

$$\varphi_S(x_1, x_2, x_3, t) = \frac{1}{R} \cos\left(\frac{K}{B} R\right) \exp\left(iK \frac{M_\infty}{B} x_1\right) \exp(i\omega t) \quad . \tag{3.19}$$

To evaluate the velocity potential for the delta wing with supersonic leading edges, one can consider a continuous distribution of pulsating sources on the surface of the wing. At a point on the plane of the wing, $P(x_1, x_2, x_3 = 0)$, the velocity potential can thus be expressed in the form

$$\hat{\varphi}(x_1, x_2, x_3 = 0) = -\frac{1}{\pi} \int\int_{wing} \hat{W}(x_{1S}, x_{2S}) \exp(-ikX) \cos\left(\frac{k}{M_\infty} X \bar{R}\right) \frac{dX dY}{\bar{R}} \quad , \tag{3.20}$$

where X , Y and $\bar{R}$ are defined by the equations

$$X = x_1 - x_{1S} \quad , \quad Y = \frac{x_2 - x_{2S}}{x_1 - x_{1S}} \quad , \tag{3.21}$$

$$\bar{R} = \frac{R}{X} \quad \Rightarrow \quad \bar{R} = \sqrt{1 - Y^2} \quad , \quad \frac{dx_1 dx_2}{R} = \frac{X dX dY}{X \bar{R}} = \frac{dX dY}{\bar{R}} \quad . \tag{3.22}$$

In this work, in equation (3.20) the integration in X is performed analytically and the integration in Y is evaluated semi-analytically. For conciseness, the steps related to these integral evaluations are not shown here (see Reference [9] for details).

The final expression in complex form of the reduced pressure coefficient on the wing can be obtained from equation (3.11) as

$$\hat{C}_p(x_1, x_2, 0) = 2 \left[(k + \lambda) \hat{\varphi} \sin(kx_1) - \frac{\partial \hat{\varphi}}{\partial x_1} \cos(kx_1)\right] - 2i \left[(k + \lambda) \hat{\varphi} \cos(kx_1) + \frac{\partial \hat{\varphi}}{\partial x_1} \sin(kx_1)\right], \tag{3.23}$$

where $\hat{\varphi}$ and its derivative with respect to x_1 are obtained by performing the integration in equation (3.20) as mentioned above.

The unsteady pressure coefficient on the wing can now be obtained by taking the real part of the equation (3.10) in the form

$$C_p(x_1,x_2,0,t) = Re\left\{\hat{C}_p(x_1,x_2,0)\right\}\cos(\omega t) - Im\left\{\hat{C}_p(x_1,x_2,0)\right\}\sin(\omega t) \quad , \tag{3.24}$$

Since the right-hand side of equation (3.9) has been evaluated accurately via the pulsating sources, the solution for the unsteady pressure coefficient obtained here is more accurate than the approximate solution presented in Reference [7].

3.2 Generalized forces due to aerodynamic loading

The generalized force $\{Q_{aero}\}$, due to the unsteady supersonic aerodynamic loading on the delta wing, is calculated in this section based on the unsteady pressure distribution determined in Section 3.1.

It is assumed that there is a flexular oscillation of the plane wing. The small structural displacement at any point on the wing, denoted by h in the previous Section 3.1 in equation (3.4), is set equal to w of equation (2.4). Hence $\hat{h}$ can be written as

$$\hat{h} = \sum_{r=1}^{M}\sum_{s=1}^{N}\Phi_r(x_{2s})\Psi_s(x_{1s})\hat{q}_{rs} \quad , \tag{3.25}$$

where Φ_r and Ψ_s are the chosen shape functions as defined by equations (2.7) and (2.8), respectively, and $\hat{q}_{rs}$, are the reduced generalized displacements defined as

$$\hat{q}_{rs} = q_{rs}/\exp(i\omega t) \quad , \tag{3.26}$$

where ω is the radian frequency of the wing oscillation. The chosen shape functions are rewritten in terms of the new coordinates X, Y , and the reduced velocity potential is then solved and the reduced coefficient of pressure, $\hat{C}_p$, for the aerodynamic loading on the wing structure is obtained as discussed in the previous section.

The pressure distribution for the upper surface of the wing is now given by the following:

$$p(x_1,x_2,t) = \tfrac{1}{2}\rho_\infty U_\infty^2 \hat{C}_p(x_1,x_2)\exp(i\omega t) + p_\infty \quad , \tag{3.27}$$

where ρ_∞ is the density of the free stream and p_∞ is the free stream pressure. Since $\hat{C}_{p,lower} = -\hat{C}_{p,upper}$, the net pressure on the wing can be written as

$$\Delta p(x_1,x_2,t) = \rho_\infty U_\infty^2 \hat{C}_p(x_1,x_2)\exp(i\omega t) \quad . \tag{3.28}$$

The pressure difference distribution given by equation (3.28) represents the aerodynamic loading on the wing. Therefore, the generalized forces due to this aerodynamic loading in non-dimensional form can be written as

$$\{Q_{aero}\} = \sum_{m=1}^{M}\sum_{n=1}^{N}\int_0^1\int_0^{(1-\xi)} \rho_\infty U_\infty^2 C_p(x_1,x_2,t)\,\Phi_m(\xi)\Psi_n(\eta)\,lc\,d\xi\,d\eta \tag{3.29}$$

where $\Phi_m(\xi)$ and $\Psi_n(\eta)$ are as defined by equations (2.7) and (2.8), respectively.

$\{Q_{aero}\}$ is a complicated function of ω and t . Hence it cannot he broken down into simple coefficients of 1, ω and ω^2. In other words, matrix [A] in the state-space equation (2.14), for the present case is very complicated. However, we can still solve for these generalized forces by first defining the generalized displacements using equation (3.26) as

$$\{\tilde{q}_{rs}\} = [\{q^c_{rs}\}\cos\omega t + \{q^s_{rs}\}\sin\omega t] + i\,[\{q^c_{rs}\}\sin\omega t - \{q^s_{rs}\}\cos\omega t] \tag{3.30}$$

where '$\sim$' above $\{q_{rs}\}$ indicates that both the real and imaginary components of the generalized displacements are present.

$\{Q_{aero}\}$ can be written in terms of the real and imaginary parts of the reduced potential and reduced velocity. Hence, the equation for generalized forces, equation (3.29), is rewritten as the following:

$$\{Q_{aero}\} = Re\,[\,[Z_R(\omega)]\{\tilde{q}_{rs}\} + i\,[Z_I(\omega)]\,]\{\tilde{q}_{rs}\} \quad . \tag{3.31}$$

In the above equation, $[Z_R(\omega)]$ and $[Z_I(\omega)]$ are matrices of size MN x MN and their elements are given by

$$Z_{R_{mn,rs}} = \int_0^1 \int_0^{(1-\xi)} \rho_\infty U_\infty^2 D_{R_{rs}} \Phi_m(\xi)\Psi_n(\eta)\, lc\, d\xi\, d\eta \quad , \tag{3.32}$$

$$Z_{I_{mn,rs}} = \int_0^1 \int_0^{(1-\xi)} \rho_\infty U_\infty^2 D_{I_{rs}} \Phi_m(\xi)\Psi_n(\eta)\, lc\, d\xi\, d\eta \quad , \tag{3.33}$$

where

$$D_{R_{rs}} = -\frac{1}{\pi}\cos(kx_1)\,[\hat{\varphi}_R + \hat{u}_R] \quad , \tag{3.34}$$

$$D_{I_{rs}} = -\frac{1}{\pi}\sin(kx_1)\,[\hat{\varphi}_I + \hat{u}_I] \quad . \tag{3.35}$$

In equations (3.34) and (3.35) $\hat{\varphi}$ and $\hat{u} = \partial\hat{\varphi}/\partial x_1$ are the reduced potential and the reduced velocity respectively obtained from equation (3.20) and subscripts R and I indicate their real and imaginary parts. Equations (3.32) and (3.33) are evaluated numerically as described in Reference [9]. Finally, substituting equation (3.30) into equation (3.31), one obtains

$$\{Q_{aero}\} = [Z_R(\omega)][\{q^c_{rs}\}\cos\omega t + \{q^s_{rs}\}\sin\omega t] - [Z_I(\omega)][\{q^c_{rs}\}\sin\omega t - \{q^s_{rs}\}\cos\omega t] \quad . \tag{3.36}$$

Hence the generalized forces due to aerodynamic loading have now been obtained.

4 Piezoelectric modelling

In principle, piezoelectric actuators can be introduced on the wing in order to reduce the aeroelastic oscillations of the wing. The piezoelectric actuators are modelled here as PVDF strips bonded to the wing and the following assumptions are made:

1. PVDF strips are homogeneous, isotropic and are perfectly bonded to the structure;
2. Thicknesses of all the PVDF strips are constant; and
3. Strips are polarized so as to produce uni-directional strains.

A trapezoidal shape for the PVDF strips is chosen because they are simpler to manufacture than an irregular geometry. Trapezoidal strips also cover triangular plates better than rectangular strips would. Let subscript 'i ' refer to the i th PVDF strip, $i = 1,2,\ldots,R_t$ where R_t is the total number of strips covering the wing.

Strips aligned in the x-direction are described by a shape function $f(x)$ polarized to expand and contract in the x-direction. Mathematically [9],

$$b_i(x) = b_i(x_i) f(x) \quad , \tag{4.1}$$

where

$$f(x) = 1 + [\{b_i(x_i + a_i) - b_i(x_i)\} / a_i b_i(x_i)] \ [x - x_i] \quad , \tag{4.2}$$

in which, as shown in Figure 3(a), $b_i(x)$ is the width of the PVDF strip at any location along the x-axis, $b_i(x_i + a_i)$ is the minimum width of the PVDF strip, and $b_i(x_i)$ is the maximum width of the PVDF strip.

Similarly, a strip aligned in the y -direction, for example the strip 2 in Figure 1, is polarized to expand and contract in the y -direction. The shape distribution function,$g(y)$, for strips polarized in the y -direction is defined as

$$a_i(y) = a_i(y_i) g(y) \quad , \tag{4.3}$$

where

$$g(y) = 1 + [\{a_i(y_i + b_i) - a_i(y_i)\} / b_i a_i(y_i)] \ [y - y_i] \quad , \tag{4.4}$$

in which $a_i(y)$ is the width of the PVDF strip at any location along the y-axis as shown in Figure 3(b).

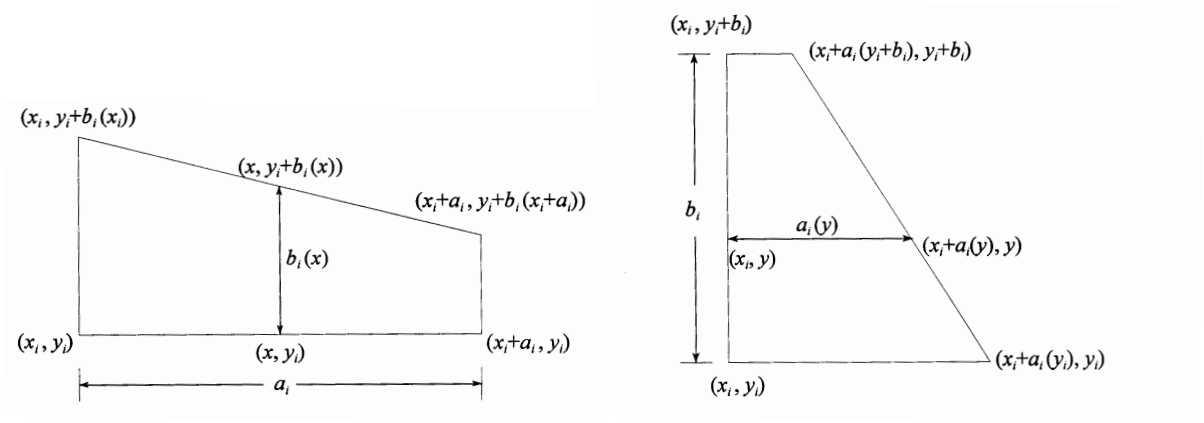

Fig. 3 (a) Shape of PVDF strip polarized in the x -direction. (b) Shape of PVDF strip polarized in the y-direction.

Consider an elemental area of the composite element shown in Figure 4. When the polarization is in the x -direction, the tension per unit width is

$$T(x) \propto V_{ix}(t) f(x) \quad , \tag{4.5}$$

where $f(x)$ is given by equation (4.2) and $V_{ix}(t)$ is the voltage applied across the thickness of the $i-$ th strip polarized in the x -direction. Similarly, when the force is in the y -direction, the tension per unit width is

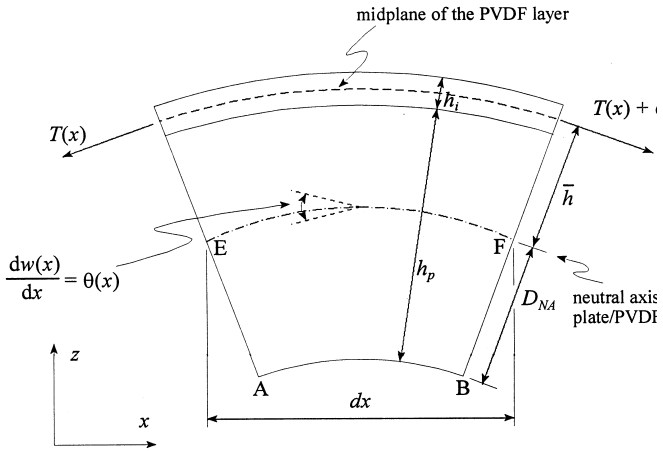

Fig. 4 Cross-section of an infinitesimal plate element area.

$$T(y) \propto V_{iy}(t)g(y) \tag{4.6}$$

where $g(y)$ is given by equation (4.4) and $V_{iy}(t)$ is the voltage applied across the thickness of the $i-$ th strip polarized in the y-direction. The tensions, $T(x)$ and $T(y)$ induce the moments $M(y)$ and $M(x)$, respectively.

Now the rate of work done by the bending moment produced by the tension acting on the elemental area is given by

$$dP = \dot{\theta}_y \bar{h} \left[\left(\frac{\partial T}{\partial x} dx \right) dy \right] + \dot{\theta}_x \bar{h} \left[\left(\frac{\partial T}{\partial y} dy \right) dx \right] \quad , \tag{4.7}$$

where $\bar{h}$ is the moment arm that acts through the elemental area as shown in Figure 4.

Also,

$$\dot{\theta}_x = \frac{\partial}{\partial t} \left(\frac{\partial w}{\partial y} \right) \qquad \text{and} \qquad \dot{\theta}_y = \frac{\partial}{\partial t} \left(-\frac{\partial w}{\partial x} \right) \tag{4.8}$$

where w is the transverse displacement given by equation (2.4). The rate of work done on an elemental area of the wing covered by the strips can now be expanded [9] and written as

$$dP = \bar{c}_{xi} V_{ix}(t) f'(x) \dot{\theta}_y \, dxdy - \bar{c}_{yi} V_{iy}(t) g'(y) \dot{\theta}_x \, dxdy \tag{4.9}$$

where $\bar{c}_{xi}$ and $\bar{c}_{yi}$ are referred to as the equivalent stiffness coefficients. These coefficients are constant per unit width with units of N/volt and they depend on the material properties and dimensions of the strip. The coefficients can be shown to be

$$\bar{c}_{xi} = E_i \{ (h_p + h_i)/2 \} d_{31} \quad , \quad \bar{c}_{yi} = E_i \{ (h_p + h_i)/2 \} d_{32} \quad , \tag{4.10}$$

where h_p is the thickness of the plate, h_i is the thickness of the ith PVDF strip, E_i is the Young's Modulus of the strip, and d_{31} and d_{32} are the piezoelectric constants for the strips polarized in the x - and y -directions, respectively.

Assume that the strips are unipolar. That is, at any given time a strip is polarized either in the x -direction or in the y -direction, but not both. The total power acting on the total area covered by the strips can now be written as

$$P = \{1\}^T \left\{ \tilde{P} \right\} \quad , \tag{4.11}$$

where $\{1\}$ is a (R_t x 1) unit vector and

$$\left\{\tilde{P}\right\} = [P_x]\{V_{ix}(t)\} + [P_y]\{V_{iy}(t)\} \quad . \tag{4.12}$$

The power components from this equation can be written as

$$P_{x_{irs}} = \tilde{c}_{xi}\Omega_{irs} \quad , \quad P_{y_{irs}} = \tilde{c}_{yi}\zeta_{irs} \quad , \tag{4.13}$$

where

$$\Omega_{irs} = -\int_{\xi_i}^{\xi_i + a_i/l} \int_{\eta_i}^{\eta_i + \tilde{b}_i(\xi_i)} f'(\xi)\left[\partial\left\{\Phi_r(\xi)\Psi_s(\eta)\right\}/\partial\xi\right](c/l)(1-\xi)\, d\xi\, d\eta \quad , \tag{4.14}$$

$$\zeta_{irs} = -\int_{\eta_i}^{\eta_i + b_i/c} \int_{\xi_i}^{\xi_i + \tilde{a}_i(\eta_i)} g'(\eta)\left[\partial\left\{\Phi_r(\xi)\Psi_s(\eta)\right\}/\partial\eta\right]\left[l/c\,(1-\xi)\right] d\eta\, d\xi \quad , \tag{4.15}$$

in which the limits are $\tilde{b}_i(\xi_i) = b_i(x_i)/c$ and $\tilde{a}_i(\eta_i) = a_i(y_i)/l$, respectively. The dimensions of the matrices on the right side of equation (4.12) are

$$\dim[P_x] = MN\ x\ R_t \quad , \quad \dim\{V_{ix}(t)\} = R_t\ x\ 1 \quad , \tag{4.16}$$

$$\dim[P_y] = MN\ x\ R_t \quad , \quad \dim\{V_{iy}(t)\} = R_t\ x\ 1 \quad . \tag{4.17}$$

Substituting equation (4.12) into the equation of motion (2.12) and rewriting it in the state-space form, equation (2.14), one obtains

$$\{\dot{x}\} = [A]\{x\} + [B_x]\{V_{ix}(t)\} + [B_y]\{V_{iy}(t)\} \quad . \tag{4.18}$$

The matrices [B_x] and [B_y] can be written as

$$[B_x] = \begin{bmatrix}[0]_x \\ [P_x]\end{bmatrix}, \quad [B_y] = \begin{bmatrix}[0]_y \\ [P_y]\end{bmatrix} \quad , \tag{4.19}$$

where $[0]_x$ and $[0]_y$ are both (MN x R_t) null matrices.

The generalized forces due to the interaction of the PVDF strips with the delta wing can now be written as

$$\{Q_{piezo}\} = [B_x]\{V_{ix}(t)\} + [B_y]\{V_{iy}(t)\} \quad , \tag{4.20}$$

Also, equation (4.18) can be further written as

$$\{\dot{x}\} = [A]\{x\} + \{Q_{piezo}\} \quad . \tag{4.21}$$

Now that the generalized forces, $\{Q_{piezo}\}$, due to the presence of the piezoelectric strips have been obtained, the transient response of the wing, which is presented in the next section, can be determined using equation (4.21). Furthermore, the dynamic response of the delta wing under unsteady, supersonic loading in the presence of these piezoelectric strips will also be presented in the next section.

5 Dynamics of the system under both piezoelectric and aerodynamic loadings

The response of the delta wing, with and without aerodynamic loading in the presence of PVDF actuators is discussed in this section. To begin with, we consider the wing under the influence of the piezoelectric strips alone. Following that, the unsteady supersonic aerodynamic loading is introduced on the wing with piezoelectric strips present. The dynamics of the system under the combined piezoelectric and aerodynamic forces are then analysed and displacements of the three points on the delta wing shown in Figure 1 are examined. The plate is assumed to be made of an aluminum alloy.

5.1 Transient response of the delta wing

In this subsection, the PVDF strips are activated to damp out the oscillations of an unloaded delta wing. In other words, equation (4.21) is solved. The structural damping, C, given by equation (2.13) is also present. Once the generalized displacements and the generalized velocities for this forced system have been determined, the response of the plate at the points under consideration can be easily determined. As shown in Figure 1, strips 1,3 and 5 are assumed to be oriented along the x-direction whiel strips 2 and 4 are assumed to be oriented in the y-direction. The matrices [B_x] and [B_y] can now be easily generated numerically. The voltage is selected as follows:

$$V_i(t) = -K_i \dot{w}_{tip} \quad , \tag{5.1}$$

where K_i is a constant and $\dot{w}_{tip}$ is the tip velocity.

Using these voltages, $\{Q_{piezo}\}$ can be determined and the state-space equation, equation (4.21) can be solved. A program was written in MATLAB to solve the state-space equations using the Runge-Kutta method. Once the generalized displacements have been determined, they are in turn placed in equation (2.4). All the components of equation (2.4) are now known and the transverse displacements, w , at the three locations shown in Figure 1 can be calculated.

5.2 Harmonic response of the delta wing

In this subsection, the procedure to obtain the dynamic response of the wing under the combined forces of the unsteady supersonic aerodynamic loading and those of the piezoelectric strips are discussed. The dynamic response of the delta wing is compared for the following two cases:

1. Forced vibrations due to piezoelectric loading (without aerodynamic loading), that is $\{Q_{aero}\} = \{0\}$.
2. With both aerodynamic and piezoelectric loading, that is $\{Q_{aero}\} \neq \{0\}$.

In both cases the piezoelectric strips are active. When $\{Q_{aero}\} \neq \{0\}$, the piezoelectric and aerodynamic forces are simultaneously acting on the wing. But when $\{Q_{aero}\} = \{0\}$, the only external force applied to the delta wing is generated by the PVDF strips. These forces are solely responsible for activating the wing oscillations. The aim of this comparison is to determine whether or not the PVDF strips can counter the wing oscillations caused by the aerodynamic loading. Specifically, it has to be demonstrated that the forces due to the piezoelectric strips can effectively oppose the aerodynamic forces, thereby reducing the aeroelastic oscillations. In other words, the magnitude of displacement of the wing has to be smaller when $\{Q_{aero}\} \neq \{0\}$ as compared to when $\{Q_{aero}\} = \{0\}$, in order to conclude that the PVDF strips are effective in controlling the aeroelastic oscillations of the delta

wing. The appropriate combinations of the strips and voltages (applied across the individual strips) to obtain effective control of the aeroelastic wing oscillations are determined by trial and error.

Now, the equation of motion for the dynamics system, equation (2.12), is rewritten as:

$$[M]\{\ddot{q}_{rs}\} + [C]\{\dot{q}_{rs}\} + [K]\{q_{rs}\} = \{Q_{aero}\} + \{Q_{piezo}\} \quad , \tag{5.2}$$

where r and s identify the shape functions in the clamped-free and free-free directions respectively, $\{q_{rs}\}$ is given by equation (3.30), and $\{\dot{q}_{rs}\}$ and $\{\ddot{q}_{rs}\}$ are the generalized velocities and accelerations respectively. $\{Q_{aero}\}$ and $\{Q_{piezo}\}$ are given by equations (3.36) and (4.20), respectively. In equation (4.20) let

$$V_{ix} = \hat{V}_{ix}^{c}\cos\omega t + \hat{V}_{ix}^{s}\sin\omega t, \quad V_{iy} = \hat{V}_{iy}^{c}\cos\omega t + \hat{V}_{iy}^{s}\sin\omega t \quad , \tag{5.3}$$

where $\hat{V}_{ix}^{c}$,$\hat{V}_{ix}^{s}$,$\hat{V}_{iy}^{c}$, $\hat{V}_{iy}^{s}$ are the voltage amplitudes introduced across the thickness of the individual piezoelectric strips.

As discussed in Section 3, the aerodynamic components of $\{Q_{aero}\}$,$[Z_R(\omega)]$ and $[Z_I(\omega)]$, are complicated functions of frequency, ω . Hence, matrix [A] in the state-space equation for the present case is complicated. Thus, for this case, we will not be able to use the Runge-Kutta method directly for integrating ordinary differential equations. The transverse displacement of the delta wing, however, can still be determined by solving for the generalized displacements. We are interested only in the real part of the generalized displacements which is given by

$$\{q_{rs}\} = Re\{\tilde{q}_{rs}\} = \{q_{rs}^{c}\}\cos\omega t + \{q_{rs}^{s}\}\sin\omega t \quad . \tag{5.4}$$

The generalized velocities and generalized accelerations are obtained by differentiating equation (5.4) with respect to time.

Substituting equations (3.36), (4.20) and (5.4) and the generalized velocities and accelerations into equation (5.2) one obtains

$$\begin{Bmatrix} q_{rs}^{c} \\ q_{rs}^{s} \end{Bmatrix} = [AB]^{-1}\{Q_{volt}\} \quad , \tag{5.5}$$

where

$$[AB] = \begin{bmatrix} [A_{11}+B_{11}] & [A_{12}+B_{12}] \\ [A_{21}+B_{21}] & [A_{22}+B_{22}] \end{bmatrix} \quad , \tag{5.6}$$

in which

$$A_{11} = -\omega^2[M] + [K] \quad , \quad A_{12} = \omega[C] \quad , \quad A_{21} = -\omega[C], \quad A_{22} = -\omega^2[M] + [K] \quad , \tag{5.7}$$

$$B_{11} = -[Z_R(\omega)], \quad B_{12} = -[Z_I(\omega)] \quad , \quad B_{21} = [Z_I(\omega)], \quad B_{22} = -[Z_R(\omega)] \quad , \tag{5.8}$$

and

$$\{Q_{volt}\} = \begin{bmatrix} [P_x] & [0] \\ [0] & [P_x] \end{bmatrix} \begin{Bmatrix} \hat{V}_{ix}^{c} \\ \hat{V}_{ix}^{s} \end{Bmatrix} + \begin{bmatrix} [P_y] & [0] \\ [0] & [P_y] \end{bmatrix} \begin{Bmatrix} \hat{V}_{iy}^{c} \\ \hat{V}_{iy}^{s} \end{Bmatrix} \quad , \tag{5.9}$$

When $\{Q_{aero}\}$ is zero, equations (5.5) and (5.9) still hold, however equation (5.6) becomes

$$[AB] = \begin{bmatrix} [A_{11}] & [A_{12}] \\ [A_{21}] & [A_{22}] \end{bmatrix} \quad . \tag{5.10}$$

Now $\{q^c_{rs}\}$ and $\{q^s_{rs}\}$ can be solved using MATLAB. The results are substituted back into Eq. (5.4) to determine the generalized displacements, $\{q_{rs}\}$. Once the generalized displacements have been determined, the transverse displacements, w , can be determined as discussed in the previous subsection. The magnitude of the voltage applied across the thickness of the piezoelectric strips is varied to achieve maximum control of the aeroelastic oscillations. The results are discussed in the next section.

6 Numerical results

This section presents the results obtained using the mathematical model presented in the previous sections.

The transient response of the delta wing is obtained for the wing thickness $h_p = 0.01$ m and $h_p = 0.02$ m. The physical characteristics of the system are given in Table 1. It is assumed that the system has an inherent damping and that all five strips are active. Let the K_i in equation (5.1) assume the values listed in Table 2.

Table 1 Physical parameters of the system

$l = 5.0$ m	$\rho = 2823$ kg/m^3	$h_i = 5x10^{-4}$ m
$c = 2.5$ m	$E_i = 60x10^9$ Pa	$E_p = 70x10^9$ Pa
$\nu = 0.334$	$d_{31} = d_{32} = 250 \times 10^{-12}$ m/volt	

Table 2 Value of K_i

Strip, i =	1	2	3	4	5
K_i =	700	1000	500	700	500

The response at Points 1 $(\xi = 1, \eta = 0)$ and 2 $(\xi = 0.45, \eta = 0)$, when $h_p = 0.01$ m, are shown in Figures 5(a) and 5(b), respectively. Similarly, the response of the wing at the two points when $h_p = 0.02$ m are shown in Figure 6. As seen in Figures 5 and 6, the system damps out faster at the wing tip when the PVDF strips are active [Figures 5(a) (ii) and 6(a) (ii)] as compared to the case when only structural damping [Figures 5(a) (i) and 6(a) (i)] is present. Similar results are obtained for Point 2 as seen from Figures 5(b) and 6(b). Thus with the introduction of the piezoelectric strips, the wing oscillations damp out faster. Comparing Figures 5 and 6, it is also observed that increasing the thickness of the wing increases the frequency of oscillation of the wing. By introducing the PVDF strips on the wing, the thicker wing damps out faster as expected. The response obtained at Point 3 $(\xi = 0.45, \eta = 0.45)$ is similar to Point 2 and, for the sake of brevity, is not presented here.

It was also observed that activating the strips oriented in the y-direction does not have a significant effect on reducing the oscillations over time. In this case, the magnitude of the wing oscillations was comparable to that of the case when only the structural damping is present. Hence, it can be safely said that activating the span-aligned strips alone is sufficient for damping out the oscillations of the wing.

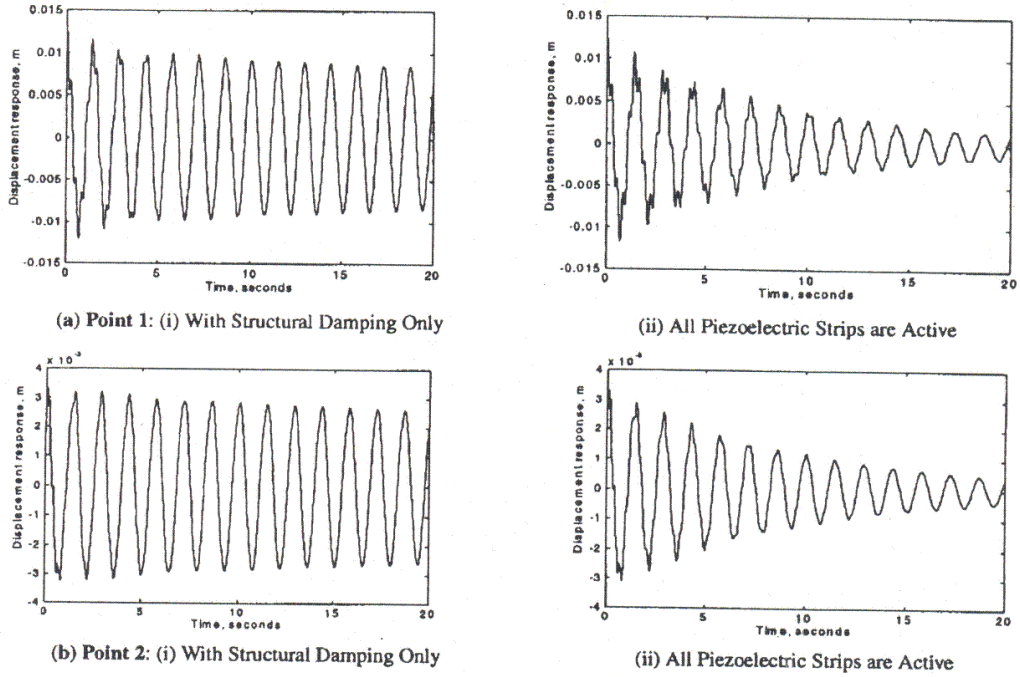

(a) **Point 1**: (i) With Structural Damping Only

(ii) All Piezoelectric Strips are Active

(b) **Point 2**: (i) With Structural Damping Only

(ii) All Piezoelectric Strips are Active

Fig. 5 Transient response of delta wing for $h_p = 0.01$ m.

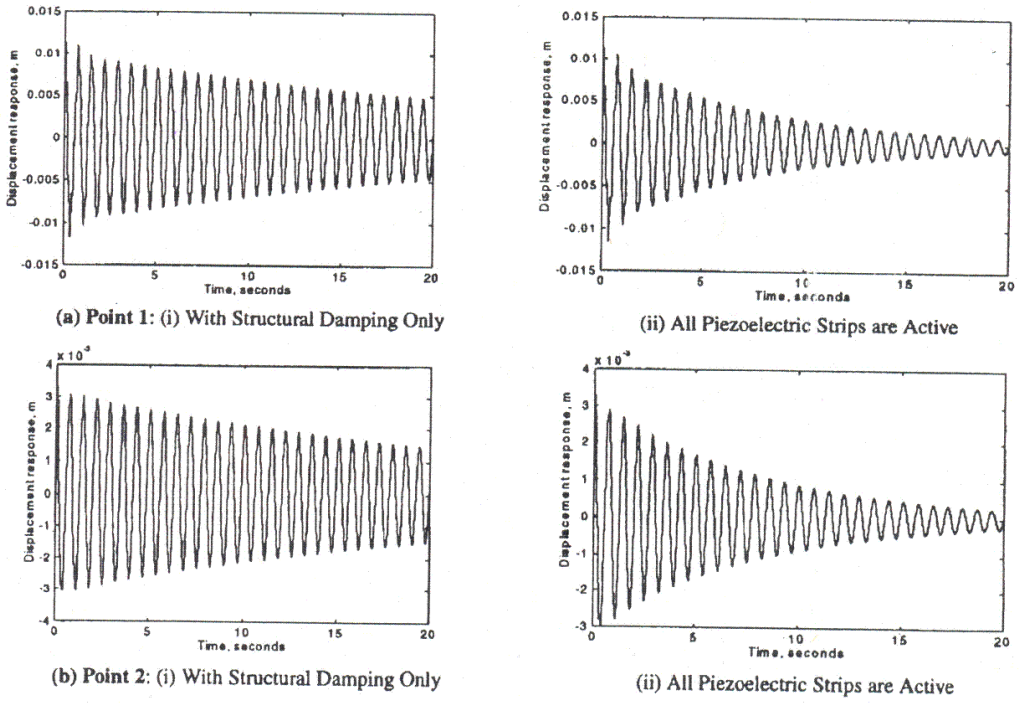

(a) **Point 1**: (i) With Structural Damping Only

(ii) All Piezoelectric Strips are Active

(b) **Point 2**: (i) With Structural Damping Only

(ii) All Piezoelectric Strips are Active

Fig. 6 Transient response of delta wing for $h_p = 0.02$ m.

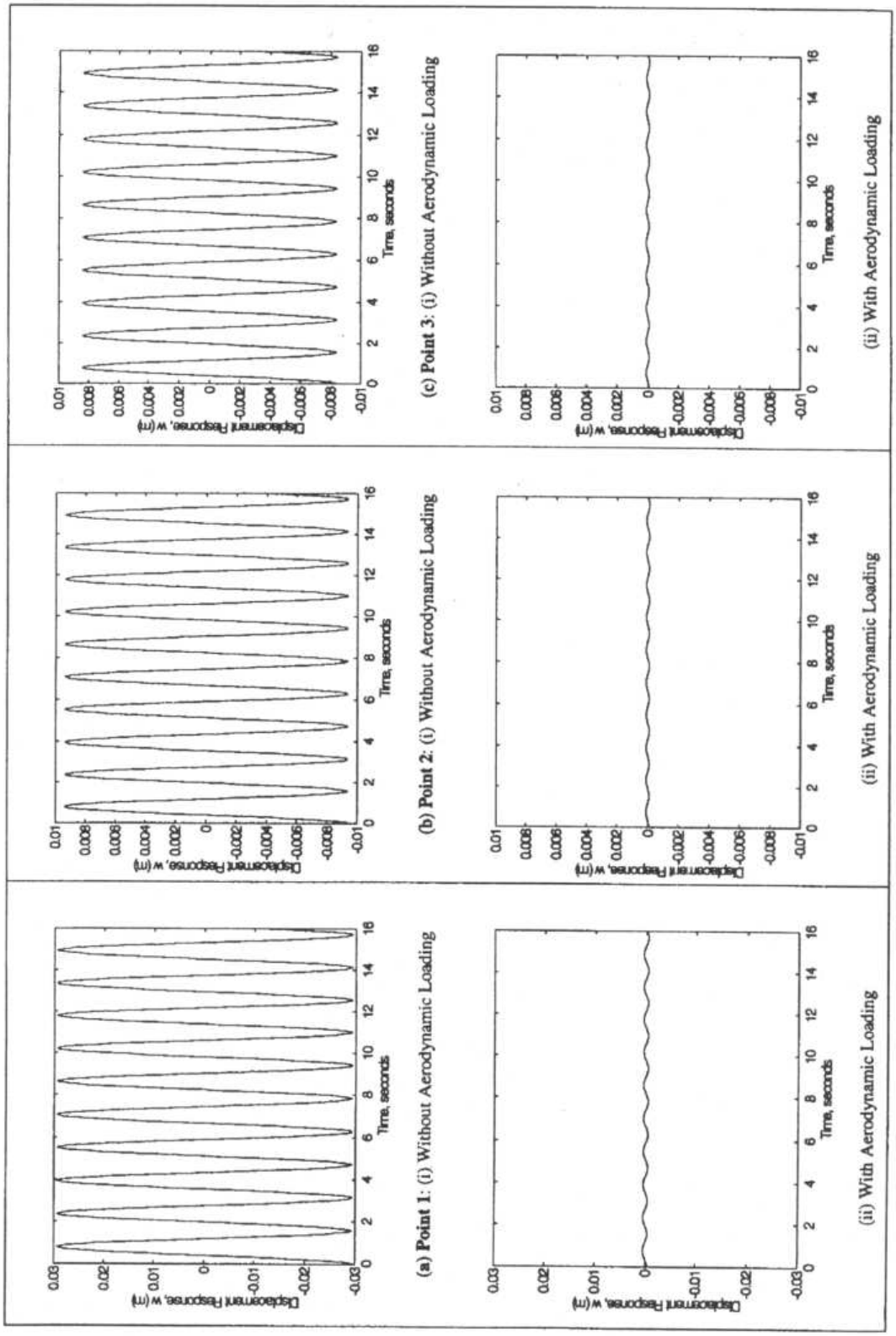

Fig. 7 Dynamic response of delta wing of thickness: $h_p = 0.01$ m. (Piezoelectric Strips are Active).

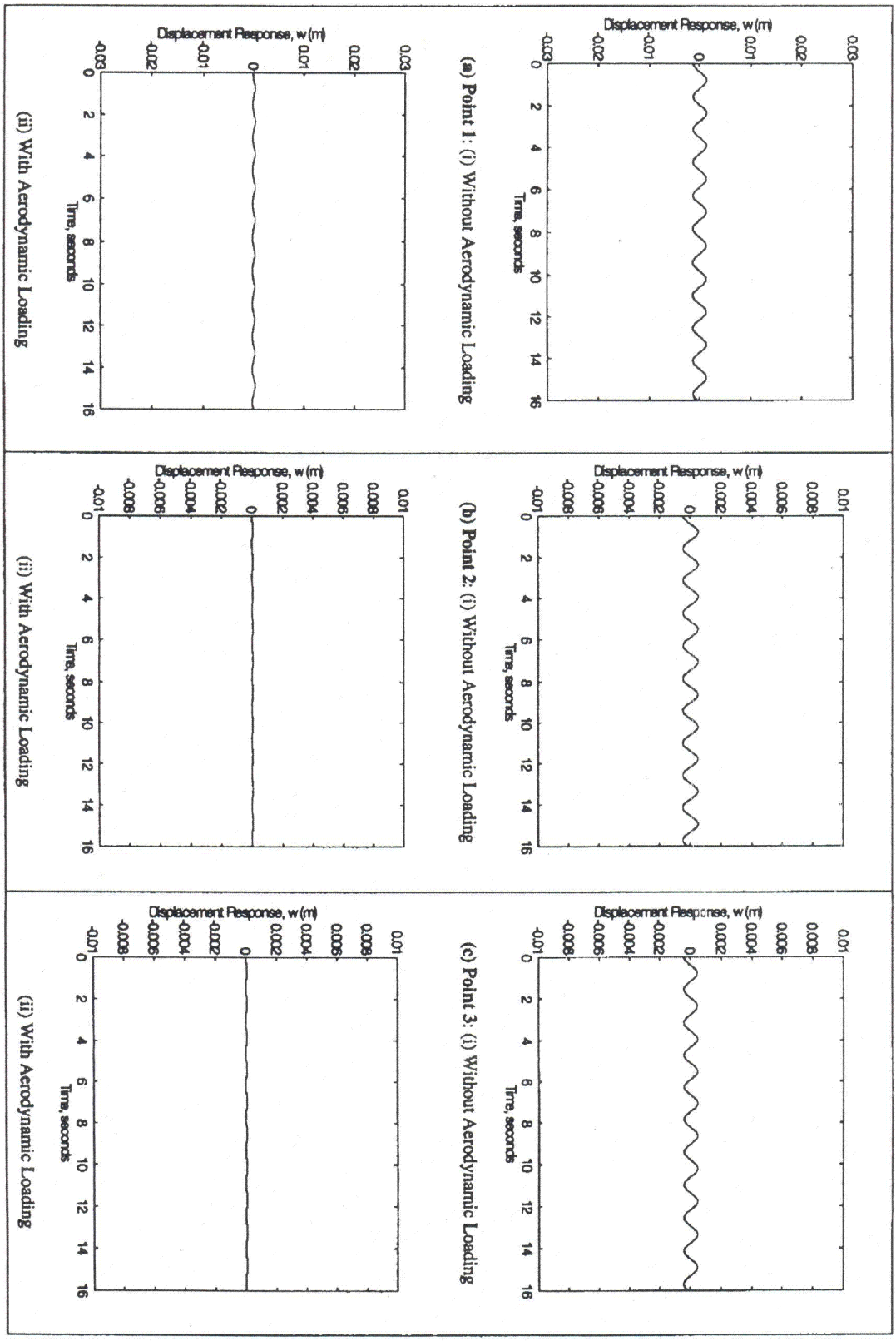

Fig. 8 Dynamic response of delta wing of thickness: $h_p = 0.02$ m. (Piezoelectric Strips are Active).

The unsteady supersonic aerodynamics loading is now introduced on this structural-piezoelectric model to study the effects of the PVDF strips in the presence of the aerodynamic loading. To obtain the response of this dynamic system, equation (5.5) is solved as was discussed earlier for the frequency ω = 4 rad/sec. A large number of numerical simulations were carried out to determine the best combinations of voltages for effective reduction of the aeroelastic oscillations. However, only a handful of results are presented herein for brevity. As a reminder, the PVDF strips are deemed useful only if the wing oscillations are smaller in magnitude when $\{Q_{aero}\} \neq \{0\}$ as compared to the case when $\{Q_{aero}\} = \{0\}$ (implying that the aerodynamic and piezoelectric effects oppose each other).

The dynamics response is again obtained for wing thickness h_p =0.01m as well as h_p =0.02 m. The voltage combination that gives the best response for the chosen periodic frequency is given in Table 3. The response is obtained at all three locations on the wing and the results are presented in Figures 7 and 8 for the two thicknesses. The figures numbered (i) represent the dynamic response of the wing when only the piezoelectric strips are acting on the wing. Similarly, the figures numbered (ii) are obtained when aerodynamic and piezoelectric forces are simultaneously acting on the wing. Comparing sets (i) and (ii) in Figures 7 and 8, it is seen that the PVDF strips effectively oppose the aerodynamic loading at all points for this voltage combination. That is, the amplitudes of delta wing oscillations at all three locations on the delta wing are reduced by more than three-fourths when aerodynamic loading is present as compared to when it is absent. This is achieved with only two active spanwise strips. Increasing the number of active strips did not produce any further significant reduction. Similar findings were reported in [2] when square anisotropic panels were studied. In the present analysis, it is again found that while the span-aligned strips contributed the most in controlling the aeroelastic oscillations, the chord-aligned strips had little or no significant effect in reducing the magnitude of wing oscillation.

Table 3 Amplitudes of voltages applied across the strips

Strip, i =	1	2	3	4	5
	$\hat{V}_{ix}^{c} = -500$	–	$\hat{V}_{ix}^{c} = -400$	–	–

From the above results it can be inferred that, with appropriate voltage application, the piezoelectric strips can oppose the aerodynamic loading on the wing, and hence effectively reduce the delta wing oscillations caused by the aerodynamic loading.

7 Conclusions

A study of aeroelastic oscillations of a delta wing under unsteady supersonic aerodynamic loading in the presence of bonded piezoelectric strips has been presented in this paper. The response of the delta wing at three locations in the presence of piezoelectric strips with and without aerodynamic loading was studied. Both transient and steady state responses were obtained for the cases when aerodynamic loading was absent. However only the steady state response was obtained for the aerodynamic loading case. In both the transient and steady state cases, it was concluded that the spanwise strips are more effective than the chordwise strips, which have little or no effect in reducing the amplitude of wing oscillations. An effective feedback control scheme was developed in the present paper for the structural-piezoelectric model, but no such feedback control scheme has been developed yet when aerodynamic loading is also present. However, from the results presented it can be seen that, with

appropriate voltages, the piezoelectric strips can oppose the aerodynamic loading on the wing and hence effectively reduce the delta wing oscillations when aerodynamics loading is present.

Appendix A

The elements of the stiffness matrix $[k]$ defined in equation (2.11) are given by

$$k_{ij} = (c/l^3) \int_0^1 \int_0^1 (k_{ij1} + k_{ij2} + k_{ij3} + k_{ij4} + k_{ij5})\, d\xi\, d\eta$$

where k_{ij1} , etc. are defined as follows:

$$k_{ij1} = (1-\xi) a_1 b_1$$

$$k_{ij2} = 4\eta a_1 b_4$$

$$k_{ij3} = [2/(1-\xi)] \left[\left\{ 2\eta^2 + k^2 (1-\nu) \right\} a_4 b_4 + \left(\eta^2 + \nu k^2 \right) a_1 b_3 + 2\eta a_1 b_2 \right]$$

$$k_{ij4} = \left[4/(1-\xi)^2 \right] \left[\left\{ 2\eta^2 + k^2 (1-\nu) \right\} a_2 b_4 + \left(\eta^3 + k^2 \eta \right) a_3 b_4 \right]$$

$$k_{ij5} = \left[1/(1-\xi)^3 \right] \left[2 \left\{ 2\eta^2 + k^2 (1-\nu) \right\} a_2 b_2 + \right.$$
$$\left. + 4 \left\{ \eta^3 + (1-\nu) k^2 \eta \right\} a_2 b_3 + \left\{ \eta^4 + k^4 + 2(1-\nu) k^2 \eta^2 \right\} a_3 b_3 \right]$$

The quantities a_i are given by

$$a_1 = (d^2\Phi_r/d\xi^2)\Psi_s + 2(d\Phi_r/d\xi)(\partial\Psi_s/\partial\xi) + \Phi_r(\partial^2\Psi_s/\partial\xi^2)$$

$$a_2 = \Phi_r(\partial\Psi_s/\partial\eta)$$

$$a_2 = \Phi_r(\partial^2\Psi_s/\partial\eta^2)$$

$$a_4 = (d\Phi_r/d\xi)(\partial\Psi_s/\partial\eta) + \Phi_r(\partial^2\Psi_s/\partial\xi\partial\eta).$$

b_i are similar to a_i except that subscripts r and s are replaced by k and$p$, respectively.

References

[1] Srinivasan, A. V. and Mcfarland, D.M., 2001, *Smart Structures: Analysis and Design*, Cambridge University Press, Cambridge, U.K.

[2] Paige, D. A., Scott, R. C., and Weisshaar, T. A., 1993, Active Control of Composite Panel Flutter Using Piezoelectric Materials, *Proceeding of Smart Structures and Materials, Smart Structures and Intelligent Systems,* Vol. 1917, SPIE, Bellingham. WA. pp. 84-97.

[3] Reich, G. W. and Crawley, E. F., 1994, Design and Modeling of an Active Aeroelastic Wing, SERC Report #4-94, Massachusetts Institute of Technology, Cambridge, MA.

[4] Lin, C. Y., Crawley, E. F., and Heeg, J., 1995, Open Loop and Preliminary Closed Loop Results of a Strain Actuated Active Aeroelastic Wing, *AIAA/ASME/ASCE/AHS/ASC 36th Structures, Structural Dynamics and Materials Conference,* pp. 1-11.

[5] Nam, C., Kim, Y., and Lee, K.-M., 1996, Optimal Wing Design for Flutter Suppression with PZT Actuators Including Power Requirement, *6th AIAA/NASA/ISSMO Symposium on Multidisciplinary Analysis and Optimization,* Part 1, Bellevue, WA, pp. 36-46.

[6] Suleman, A. and Venkayya, V. B., 1996, Flutter Control of an Adaptive Laminated Composite Panel with Piezoelectric Layers, *6th AIAA/NASA/ISSMO Symposium on Multidisciplinary Analysis and Optimization,* Part l, Bellevue, WA, pp. 141-151.

[7] Carafoli, E., Mateescu, D., and Nastase, A., 1969, Wing Theory in Supersonic Flow, 1st Edition, Pergamon Press, Oxford.

[8] Mateescu, D., 2004, Unsteady Aerodynamics, Course Notes, McGill University, Montreal, Canada.

[9] Shrivastava, S., 1998, Aeroelastic Oscillations of a Delta Wing with Bonded Piezoelectric Strips, M.Eng. Thesis, McGill University, Montreal, Canada.